Lasers in Manufacturing Conference 2019

Productivity optimization of scanner based laser ablation processes with adaptive scan paths

Matthias Buser[a,*], Daniel Holder[a], Steffen Boley[a], Volkher Onuseit[a], Thomas Graf[a]

[a]*Institut für Strahlwerkzeuge (IFSW), University of Stuttgart, Pfaffenwaldring 43, 70569 Stuttgart, Germany*

Abstract

In this study, productivity optimization was investigated for laser based ablation processes with online depth control using a fast scan path generation algorithm. In ablation processes, a depth control system utilizing optical coherence tomography can be implemented to improve geometrical accuracy and reduce surface roughness. The actuating variable for the control loop is pulse energy, which in the simplest case involves switching laser pulses on and off along the initial scan path as required. However, every suppressed pulse contributes to a decrease in productivity, which is a critical criterion for industrial applications. For this reason, an approach was taken to deploy the scan path as an additional actuating variable. The developed algorithm is designed for improving the scan path during the process by omitting already finished areas. Theoretical verification with sample geometries shows a significant improvement in productivity compared to bare pulse toggling.

Keywords: Laser ablation; tool path planning; system technology; process control

1. Introduction

Laser ablation as considered in this work is a process in which a galvo scanner unit guides the laser beam along a scan path over the work piece to create a cavity in the surface with a predefined shape. For inhomogeneous or composite materials like carbon fiber reinforced plastics (CFRP), this process shows fluctuations in material removal rate, resulting in major depth variations after a constant number of laser

* Corresponding author: Tel.: +49 711 685 60371.
E-Mail address: matthias.buser@ifsw.uni-stuttgart.de.

pulses. Consequently, precise ablation with a conventional process is not possible for such materials, as shown by Boley et al., 2017 and Dittmar et al., 2018.

In 2014, Webster et al. and in 2016, Yin et al. utilized optical coherence tomography (OCT) as an in-situ depth measurement system to add closed-loop feedback control into ablation processes. As an example, Webster showed results for precise ablation of a 3D-spiral structure in bone, a highly inhomogeneous material. This approach was later adapted by Boley et al., 2017 for ablation processes with galvo scanners on CFRP material. In this work, an OCT light source was used with a bandwidth (1060-1100 nm) close to the processing laser's wavelength (1047 nm). The two sources were combined coaxially before entering the scanning unit (see Fig. 1).

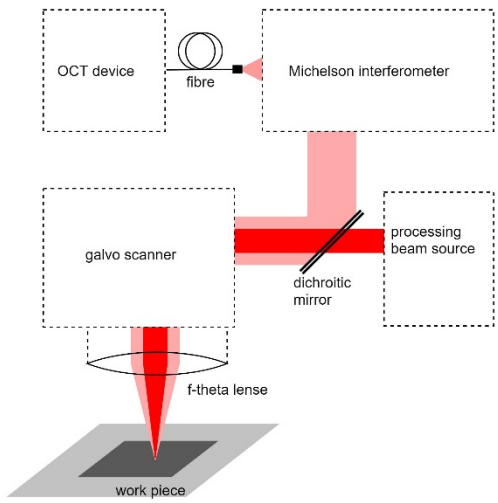

Fig. 1. Schematic of the system for depth-regulated ablation.

The depth-regulation proposed by Boley et al., 2017 is implemented as an iterative control loop. A rectangular grid is fitted around the ablation geometry subdividing the surface into pixels. Every pixel represents a depth measurement, for which the depth is compared to the target depth. Based on the depth difference, a decision is made whether further ablation is needed. The laser power is then modulated accordingly along the initial scan path. As shown by the Boley et al., 2017 this approach can provide major improvements in terms of accuracy compared to conventional ablation processes without a feedback loop.

One drawback of using only laser power modulation as the actuating variable is a decreasing degree of utilization

$$\eta_u = \frac{t_{LaserOn}}{t_{Scan}} \tag{1}$$

towards the end of the process. t_{LaserOn} represents the total time, whenever ablation takes place during a single pass and t_{Scan} represents the entire duration of a single scan pass. In Fig. 2, the progress of a depth-regulated ablation process in CFRP is shown. With increasing number of iterations, a growing portion of the initial geometry reaches target depth. For every segment that has reached target depth, the laser power is switched off on pass as specified by the iterative control loop, hence t_{LaserOn} decreases. Since the scan path does not change during the process and therefor t_{Scan} remains constant, η_{u} decreases proportionally. The

decline in η_u can be observed in this case, even though the target depth was set constant for the entire geometry. This originates from the varying material removal rate due to inhomogeneous fiber matrix distribution among the material.

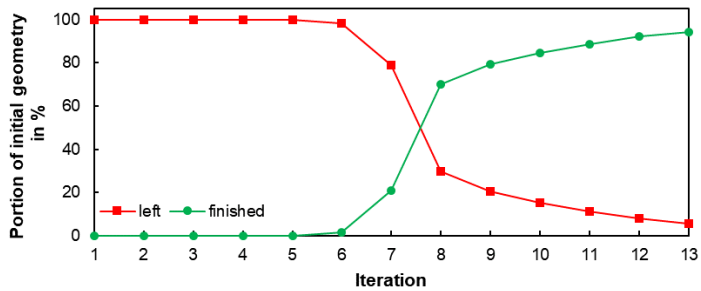

Fig. 2. Evolution of the area left to be processed as portion of the entire inital geometry. 10 by 10 mm² in CFRP, target depth 1 mm.

The goal of this work is to reduce the described decline of η_u and therefor optimizing the total processing time. From (1) it is clear, that t_{Scan} has to decrease corresponding to $t_{LaserOn}$. The approach is utilizing the scan path as an additional actuating variable for the depth-control loop. This results in an automatic adjustment of the scan path in process, so that it only covers areas, where processing is still necessary. To achieve this goal, an algorithm for scan path generation was developed.

2. Scan path generation

The main requirement for the scan path generation is to be appropriately fast for utilization in process. This excludes excessive optimization iterations and a trade-off has to be found between the benefit in terms of η_u and the time required for scan path generation. In Fig. 3 (b), a CFRP sample is shown produced by a depth-regulated process as well as one exemplary ablation geometry (a) from that process. The geometry obtained by the in-process topography measurement consists of many voids and separate islands, some with a size of only a few pixels or less, as seen in Fig. 3 (a). This prohibits the application of standard strategies for scan path generation, which optimize the scan path within every independent shape separately. If there are many separate shapes in one geometry, the movement in between, including a possibly necessary change in scan direction, will become a dominant factor in unproductive time.

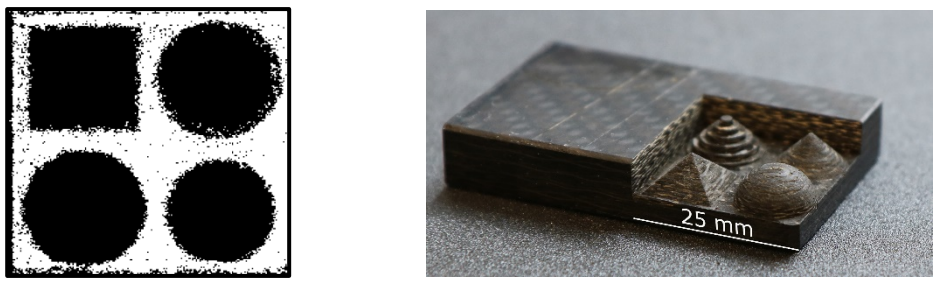

Fig. 3. (a) Ablation geometry, white with black background, 224 by 212 pixel, as occurred during the depth-regulated processing of the CFRP sample on the right (b). Every white pixel represents a spot where ablation is still required according to the OCT topography measurement.

A widely used strategy to cover shapes with a scan path is a parallel line scan (hatching) like shown by Daniel et al., 2016 or Kim et al., 2009. To improve processing time, it is critical to set the hatching angle with regard to a minimal number of lines, as stated by Hon et al., 2001. The approach in this study for fast scan path generation for complex geometries is to consider only the rough shape for the scan path and use the fast power modulation for passing voids and jumping between islands. The algorithm to find suitable hatching angles is based on the Radon transform (see Radon, 1917 or Toft, 1996) as shown in Fig. 4.

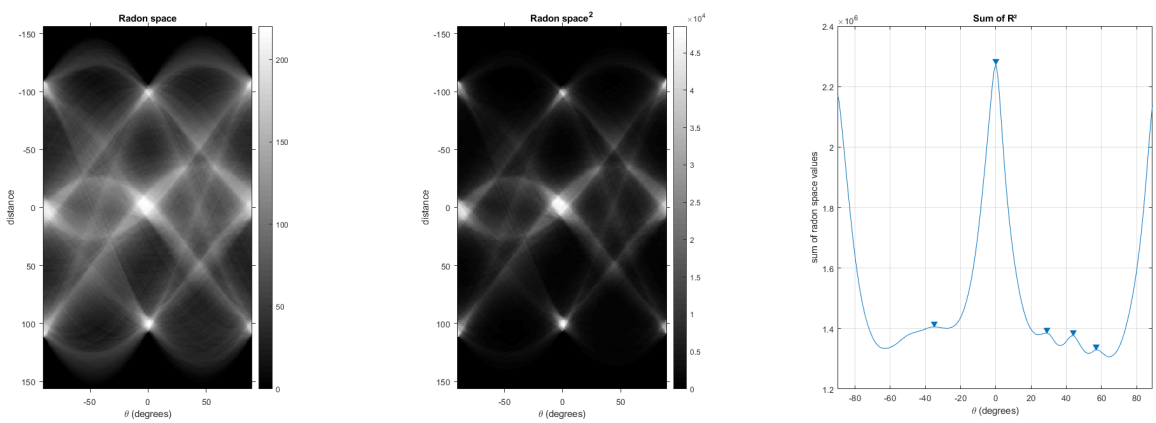

Fig. 4. three-step process of extracting promising angles for fast hatching from the geometry in Fig. 3; (a) Radon transform of geometry; (b) Squared Radon space; (c) Integral of squared Radon space over distance

It takes three steps to identify the suitable hatching angles:

1. Converting geometry from spatial domain to Radon space using Radon transform (a).
2. Squaring the Radon space (b).
3. Summing up modified Radon space over distance (c).

The resulting curve in Fig. 3 (c) shows significant peaks (0° and 90°/-90°) where few parallel lines cover major parts of the geometry. Therefore, these peaks indicate suitable hatching angles, where parallel scan lines can be fitted into the geometry.

3. Results

The described algorithm was implemented in MATLAB R2018a to calculate the scan path and the corresponding processing time for an arbitrary input geometry, considering parameters for a galvo scanner and f163 mm lens, see Table 1.

Table 1. Test parameters for a galvo scanner with f163 mm lens.

Parameter	Value
Processing speed	1 m/s
Jump speed	10 m/s
Acceleration	10,000 m/s²
Time for one line change	700 µs
Resolution of the input geometry	100 µm/pixel

Fig. 5 shows the resulting scan path of four exemplary geometries. Processing vectors are drawn red, positioning vectors green. Turnaround movements following every line are not shown but considered with a static time interval. Fig. 5 (a) shows the resulting scan path for the geometry from Fig. 3. It can been seen, that the algorithm successfully leaves out larger areas where no processing is required anymore as intended. This becomes even more useful for geometries like shown in Fig. 5 (b), where only thin regions at the edge of the processing zone are left. Both examples also show the coverage of the rough shape by the scan path and were positioning moves (green) are used for crossing voids. Example (c) was designed to demonstrate, how the algorithm improves the scan path by using multiple hatching angles within a single shape. Finally, example (d) points out to one disadvantage of the proposed strategy. Even though the geometry has a significant void within its circular shape, the void cannot be omitted beneficially. This is a consequence of the Radon transform being fundamentally based on straight lines.

Additionally, Table 2 shows the results in numbers, comparing the proposed strategy with a simple serpentine scan path. With the investigated approach, an overall reduction of processing time of 10%-40% can be achieved depending on the geometry.

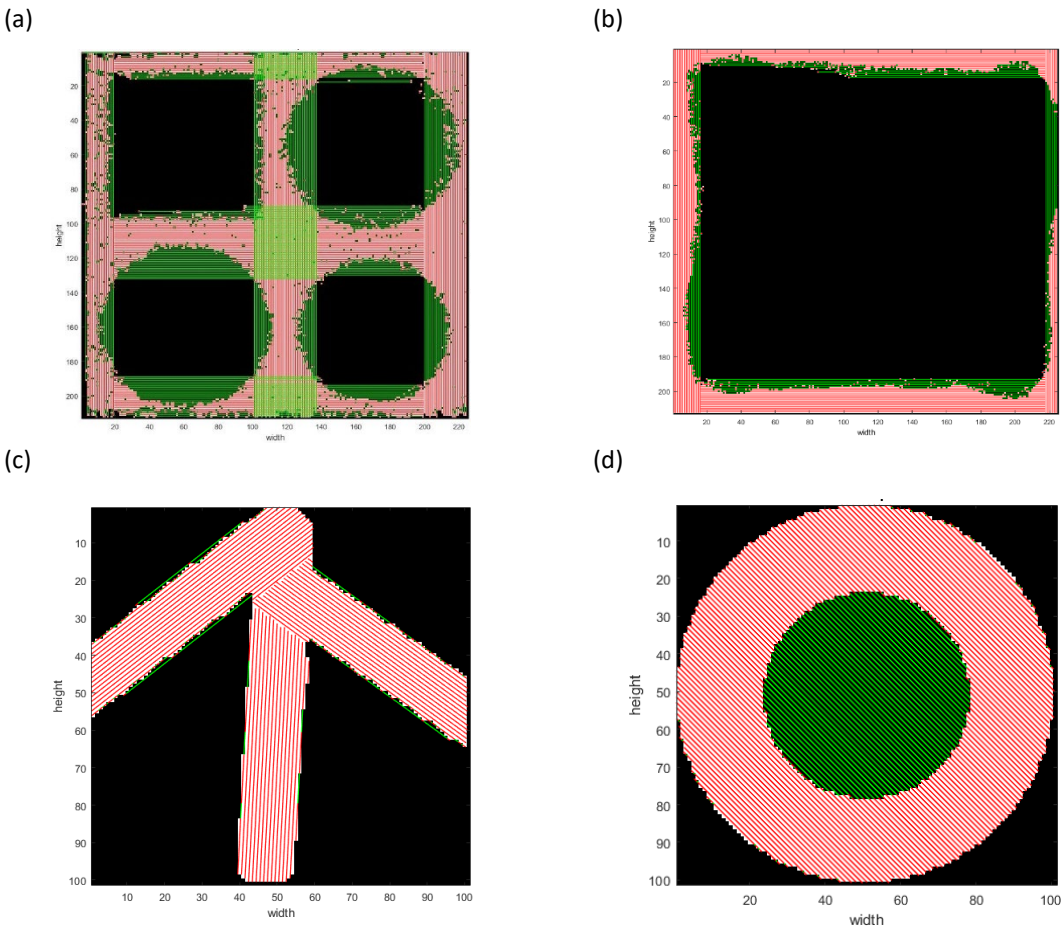

Fig. 5. Scan path as calculated by the algorithm for sample geometries. Red: Processing vector, green: Positioning vector, jumps between lines not shown

Table 2. Comparison of proposed path generation algorithm with common serpentine strategy

Geometry	Calculated scan time for serpentine strategy	Calculated scan time for proposed algorithm	reduction in processing time / increase in η_u
(a)	2,7 s	2,4 s	11%
(b)	1,6 s	1,0 s	38%
(c)	0,59 s	0,37 s	37%
(d)	0,77 s	0,69 s	10%

4. Conclusion

The proposed strategy for scan path generation calculates optimal hatching angles based on Radon transform of the geometry. Deploying the laser's property of being adjustable in power fast allows generating a scan path from parallel scan lines along the main directions of extension. With this approach, no excessive optimization is required to find scan paths also for geometries with many small voids or islands. In-process application of the algorithm seems therefor plausible. Depending on the geometry significant improvements in processing time and degree of utilization where shown. Following this work, the strategy needs to be implemented into an ablation process to investigate its impact on total processing time.

5. References

Boley, Steffen, Holder, Daniel, Onuseit, Volkher, Graf, Thomas, Buser, Matthias, Schönleber, Martin. Distance controlled laser ablation of CFRP, LiM 2017.

Daniel, C.; Manderla, J.; Hallmann, S.; Emmelmann, C. Influence of an Angular Hatching Exposure Strategy on the Surface Roughness during Picosecond Laser Ablation of Hard Materials. *Physics Procedia* 2016**,** *83*, 135–146.

Dittmar, Hagen, Jaeschke, Peter, Suttmann, Oliver, Kaierle, Stefan, Overmeyer, Ludger. Online laser-based repair preparation of CFRP supported by short coherent interferometry, LANE 2018.

Hon, M. C.; Janardan, R.; Schwerdt, J.; Smid, M. Computing Optimal Hatching Directions in Layered Manufacturing. *Computational Science — ICCS 2001*; pp 683–692.

Kim, H. C.; Lee, S. H.; Yang, S. Y. Toolpath planning algorithm for the ablation process using energy sources. *Computer-Aided Design* [Online] 2009**,** *41* (1), 59–64.

Radon, J. Über die Bestimmung von Funktionen durch ihre Integralwerte längs gewisser Mannigfaltigkeiten. *Berichte über die Verhandlungen der Königlich-Sächsischen Akademie der Wissenschaften zu Leipzig, Mathematisch-Physische Klasse* 1917**,** *69*, 262–277.

Toft, P. A. The Radon Transform: Theory and Implementation. Ph.D. Thesis; Technical University of Denmark (DTU), Denmark, 1996.

Webster, P. J. L.; Wright, L. G.; Ji, Y.; Galbraith, C. M.; Kinross, A. W.; van Vlack, C.; Fraser, J. M. Automatic laser welding and milling with in situ inline coherent imaging. *Optics letters* 2014**,** *39* (21), 6217–6220. DOI: 10.1364/OL.39.006217.

Yin, C.; Ruzzante, S. W.; Fraser, J. M. Automated 3D bone ablation with 1,070 nm ytterbium-doped fiber laser enabled by inline coherent imaging. *Lasers in surgery and medicine* 2016**,** *48* (3), 288–298. DOI: 10.1002/lsm.22459.